Physics of the Solid State, 2023, Vol. 65, No. 4

06,13

Phase composition, crystal structure, dielectric and ferroelectric properties of $Ba_2NdFeNb_4O_{15}$ thin films grown on a Si(001) substrate in an oxygen atmosphere

© A.V. Pavlenko[1], T.S. Ilyina[1,2], D.A. Kiselev[2], D.V. Stryukov[1]

[1] Southern Scientific Center, Russian Academy of Sciences,
Rostov-on-Don, Russia
[2] National University of Science and Technology MISiS,
Moscow, Russia
E-mail: Antvpr@mail.ru

Received January 27, 2023
Revised January 27, 2023
Accepted February 1, 2023

The phase composition, nanostructure, and properties of $Ba_2NdFeNb_4O_{15}$/Si(001) multiferroic thin films have been studied by X-ray diffraction analysis, scanning probe microscopy, and capacitance-voltage characteristics analysis. The RF cathode sputtering in an oxygen atmosphere was used for films fabrication. It has been found that the obtained $Ba_2NdFeNb_4O_{15}$ films are single-phase, impurity-free, polycrystalline textured (c-oriented), and the out-of-plane strain is 0.8%, which leads to the presence of ferroelectric properties at room temperature. It is shown that the surface roughness of the films is ~ 15.39 nm, the lateral size of the crystallites is ~ 134 nm, and the relative permittivity in the temperature range of $-190\ldots150^\circ$C is 95−130. The reasons for the revealed regularities are discussed

Keywords: multiferroic, dielectric characteristics, ferroelectric, tetragonal tungsten bronze.

DOI: 10.21883/PSS.2023.04.55997.13

1. Introduction

In the solid-state physics a great attention is paid to electroactive and magnetoactive materials with a structure of tetragonal tungsten bronze (TTB) with a general chemical formula of $(A1)_2(A2)_4(C)_4(B_1)_2(B_2)_8O_{30}$ [1] in the form of nanoscale films. This is due to both the prospects of their application in nanoelectronics and MEMS and the fundamental interest related to the establishing manifestation laws of dimensional effects in this type of functional structures [2]. $Ba_2LnFeNb_4O_{15}$ barium ferroniobates (where Ln is a rare-earth element) are representatives of this group of materials [3–5]. Their crystalline structure is formed by oxygen octahedra with central positions occupied by Fe^{3+} or Nb^{5+} cations, while linking of their vertices forms trigonal, tetragonal and pentagonal channels. The Ba^{2+} ions occupy pentagonal channels, the rare-earth Ln cations occupy tetragonal channels, and trigonal channels remain vacant. As for the positions in pentagonal and tetragonal channels: the crystalline structure of $Ba_2LnFeNb_4O_{15}$ multiferroic materials is filled, however, the data obtained by authors of [5,6] was indicative of the fact that vacancies are formed in Ln positions in ceramics and single-crystals in the process of synthesis, which has a significant effect on ferroelectric and magnetic properties of these materials. In the case of thin films, as known, an important role is plaid not only by the method of their synthesis but also the mechanism of their growth and their structural perfection [7], which currently is rarely analyzed in the case of ferroelectrics and multiferroics. According to the analysis of literature, $Ba_2LnFeNb_4O_{15}$ films by now are produced mainly by the following commercially used methods: the pulsed laser deposition [8], the magnetron sputtering [9] and the RF-cathode sputtering, which is being improved by us [10,11].

This study continues the studies of [10,11] and is focused on the investigation of phase composition, nanostructure, dielectric and ferroelectric properties of $Ba_2NdFeNb_4O_{15}$ (BNFNO) films grown on semiconductor silicon substrates prepared for the heteroepitaxial deposition.

2. Methods of production and investigation of samples

The $Ba_2NdFeNb_4O_{15}$ thin films were deposited on prepared single-crystal Si substrate (cut — 001, conductivity — p-type, polishing — single-side, thickness — 360 μm) by radio-frequency cathode sputtering in the oxygen atmosphere. The initial temperature of the substrate was $\sim 400^\circ$C, the oxygen pressure in the chamber was 67 Pa, the input RF-power was 150 W. The ceramic target with a stoichiometric composition of $Ba_2NdFeNb_4O_{15}$ was fabricated in the Department of Smart Materials and Nanotechnologies of Scientific Research Institute of Physics of Southern Federal University.

The X-ray diffraction studies (phase composition, structural perfection of the films, the parameters of the lattice cell and orientation relationships between

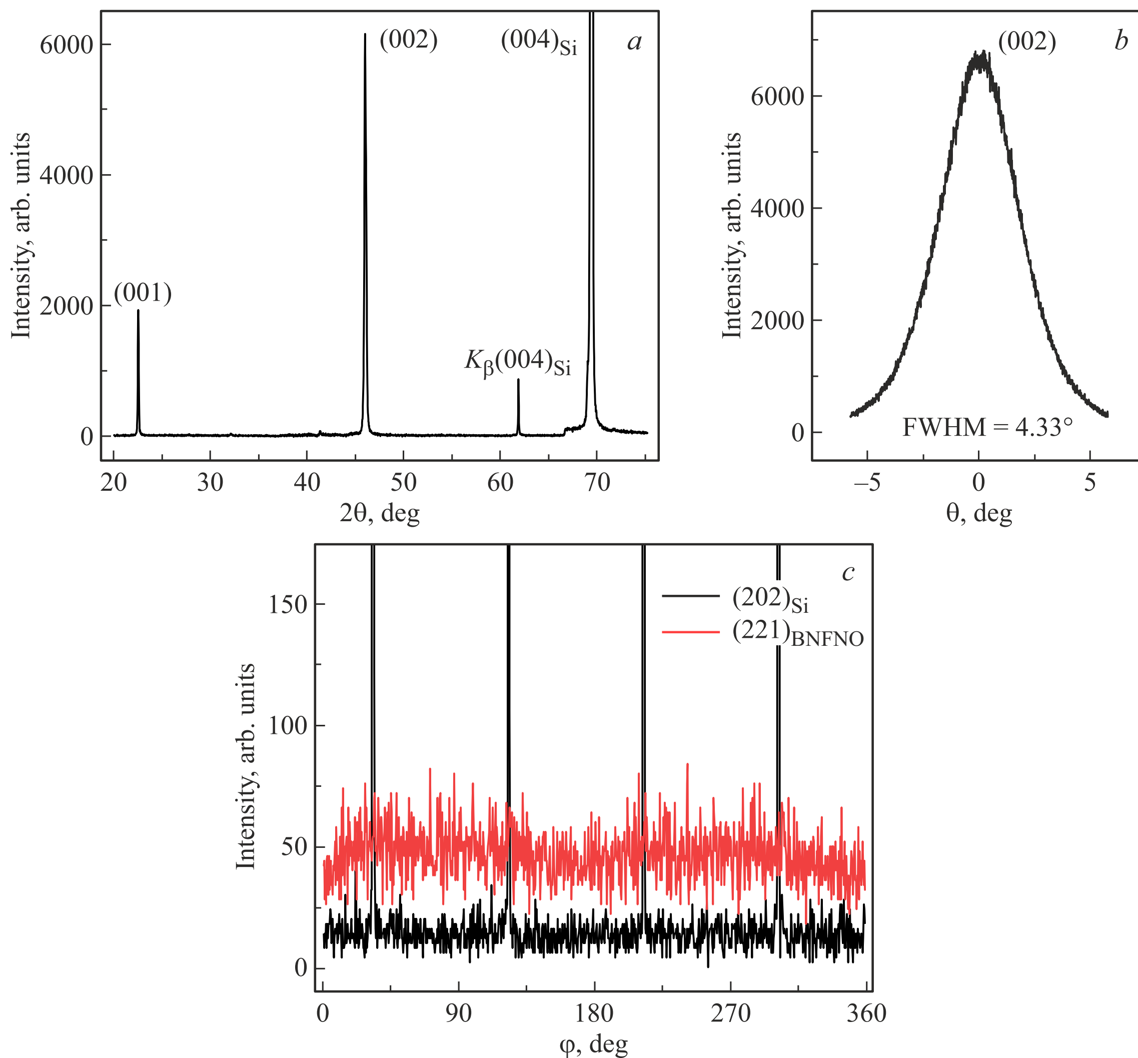

Figure 1. $\theta{-}2\theta$-X-ray pattern of the BNFNO/Si(001) heterostructure (*a*); (002) reflection rocking curve (*b*); φ-X-ray patterns of (221) reflection for the BNFNO film and (202) reflection for the Si substrate (*c*).

the film and the substrate) were carried out using the „RICOR" ($Cu_{K\alpha}$-radiation) multi-function X-ray unit. Metal–ferroelectric–semiconductor–metal (MFSM) capacitor structures were formed for dielectric measurements in the direction normal to the surface: the bottom and the top electrodes were the Ag/Pd layers deposited by magnetron sputtering in the argon atmosphere in a Emitech SC7620 unit through a mask with a hole diameter of $200\,\mu$m.

Voltage-capacitance curves ($C(U)$) at temperatures of $-190\ldots+200$°C were measured using a measurement setup included a TFAnalyzer2000 and a Linkam THMS600 stage. The heterostructure capacitance was measured at a frequency of 50 kHz at $U = 40$ mV, the triangular control voltage frequency was 1 Hz. The measurements were carried out in a measurement cell shielded against extraneous lights.

The topography, the images of domain structure, as well as the processes of local switching of the film were obtained using a Ntegra Prima (NT-MDT SI, Russia) and a MFP-3D (Asylum Research, USA) scanning probe microscopes (SPM) in the mode of piezoresponse force microscopy (PFM) with the use of NSG01Pt cantilevers (TipsNano). The images were processed and analyzed using the Gwyddion software (version 2.60).

3. Experimental results and discussion

The X-ray diffraction study has shown the BNFNO/Si(001) heterostructure has no impurity phases: $\theta{-}2\theta$ X-ray pattern in the range of 20–75° has shown only the reflections that are typical for the BNFNO film and the Si substrate (Fig. 1, *a*). Thus, for the BNFNO film, only reflections from the (00l) family of planes were observed, which is indicative of its ordered growth with the [001] axis oriented parallel to the [001] axis of the substrate. The disorientation of the [001] axis of the film determined from the rocking curve is 4.33° (Fig. 1, *b*).

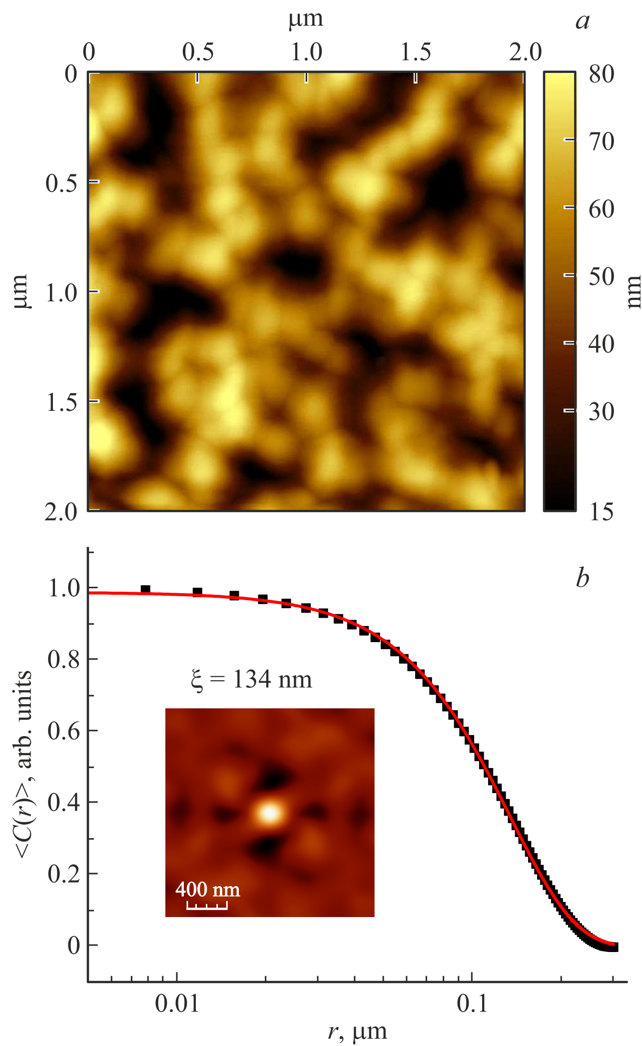

Figure 2. Topography of the BNFNO film (a), 2D-representation of the autocorrelation function of topography and curve of the radially averaged values of the medium-sized crystallites (b).

No traces of the in-plane structural ordering have been found: the φ-X-ray patterns for BNFNO show only a uniform increase in intensity independent on the φ angle, while clear maxima of (202) reflection can be seen for the single-crystal substrate (Fig. 1, c). This is indicative of the fact that the BNFNO film grown on the Si(001) substrate is a polycrystalline textured film with the [001] axis ordered in the direction of normal to the substrate plane (these structures are often referred to as „c-oriented" in literature). It is worth to note that at this stage of studies we have not succeeded in growing single-crystal BNFNO films on the Si(001) surface by varying process procedures.

The textured behavior of the BNFNO film growth has manifested through the SPM-analysis of the films (Fig. 2): the film surface is homogeneous, growth crystallites in the form of polyhedra in the horizontal plane are clearly seen, and the place of joint are predominantly flat. No inclusions of impurity phases, pores, caverns or other surface defects have been observed. Root-mean-square roughness of surface of the BNFNO film with a thickness of ~ 1000 nm was 15.39 nm. The lateral size of grains was evaluated by the method of autocorrelation function [12] in a manner similar to [13]. The 2D-representation of the autocorrelation function, which was calculated in the analysis of the results of BNFNO film surface studies, is shown in Fig. 2, b. The calculations have shown the ~ 134 nm average lateral size of the crystallites (Fig. 2, b). This all is indicative of high quality of the fabricated heterostructures.

The analysis of angular position of reflections of the BNFNO film has shown that the out-of-plane unit cell parameter c is 3.954 Å, which is considerably greater than the parameter for bulk material ($c_{\text{bulk}} = 3.923$ Å). The obtained results are indicative of the fact that even in a rather thick layers (~ 1000 nm) in the BNFNO the structure does not relax completely to the parameters of bulk sample (the tensile strain of lattice cell of the film is 0.8% compared to the bulk material), which allows expecting first a change in ferroelectric (FE) properties of the material. This is related to the fact that in $Ba_2LnFeNb_4O_{15}$ multiferroics the responsibility for the emergence of a polar state is born mainly by displacements of Fe^{3+} and Nb^{5+} cations along the four-order axis (in a nonpolar phase these cations occupy centers of octahedra) [3], and the FE-polarization arises in this direction as well. Taking this into account, properties of BFNFO films have been studied by methods of dielectric spectroscopy and SPM.

To find out the law of change in the relative permittivity $\varepsilon/\varepsilon_0$ ($\varepsilon_0 = 8.85 \cdot 10^{-12}$ F/m being dielectric constant) as a function of temperature, $C(U)$ dependencies for the Au/BNFNO/Si(001) heterostructure were measured at fixed temperatures. With the assumption that there are no interphase traps, spatial charge and other defects at the interface between the ferroelectric layer and the silicon substrate in the MFES structure, the electric induction is

$$D = \varepsilon_0 E_{\text{FE}} + P(E_{\text{FE}}) = \varepsilon_0 \varepsilon_{\text{Si}} E_{\text{Si}}, \quad (1)$$

where P is polarization of the ferroelectric and E_{FE} and E_{Si} are electric fields in the ferroelectric and the silicon substrate, respectively.

As it has been shown, for example, in [14], the relation between the surface charge density of semiconductor Q_{Si} and the field E_{Si} can be represented as $Q_{\text{Si}} = -\varepsilon_0 \varepsilon_{\text{Si}} E_{\text{Si}}$, then, taking into consideration (1), $P(E_{\text{FE}}) = -Q_{\text{Si}}$ and the semiconductor capacitance is $C_{\text{Si}} = \left|\frac{\partial Q_{\text{Si}}}{\partial C_{\text{Si}}}\right|$ (the complete representation for C_{Si} is given in [14]). It can be clearly seen that with polarization switching in FE the surface charge density of semiconductor is „tuned" and, as a consequence, the C_{Si} changes significantly. Taking into account the geometry of layers arrangement in the MFES-structure, the experimentally measured capacitance of the

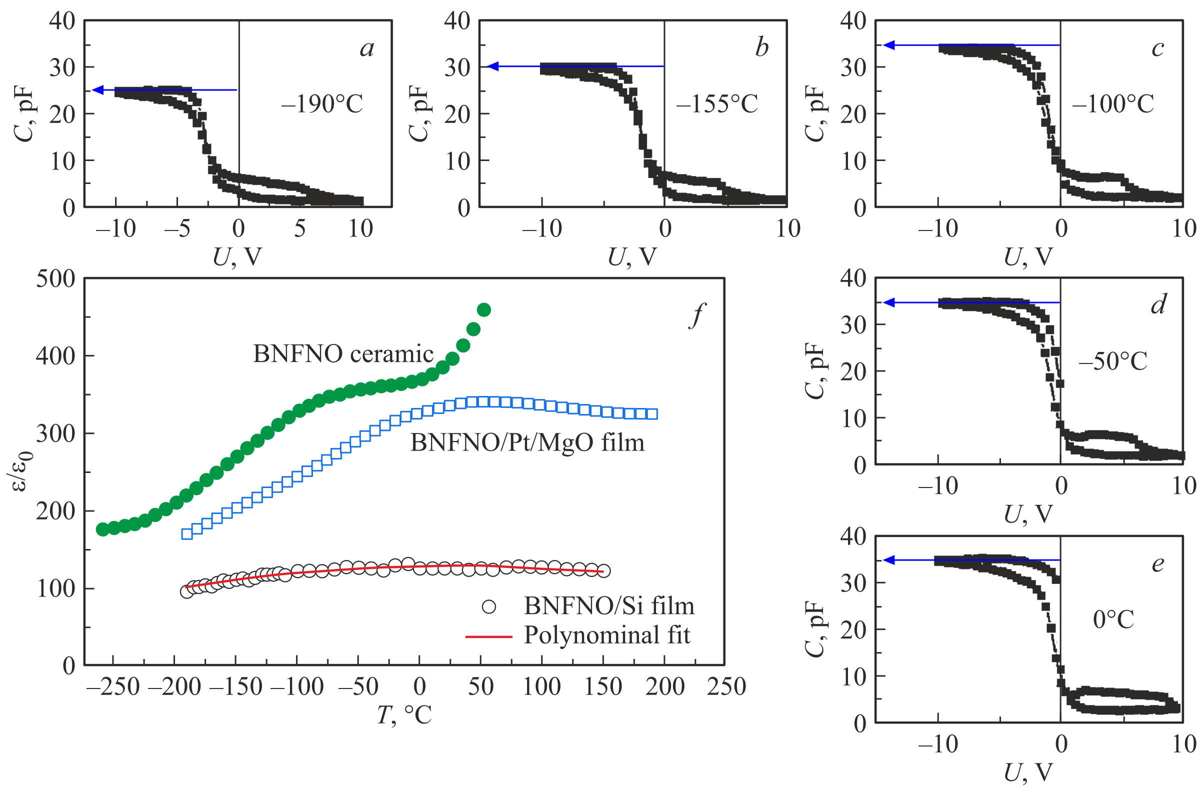

Figure 3. $C(U)$ dependence for the BNFNO/Si(001) heterostructure at -190 (*a*), -155 (*b*), -100 (*c*), -50 (*d*), 0°C (*e*); $\varepsilon/\varepsilon_0(T)$ dependencies for the BNFNO ceramics [16], BNFNO/Pt/MgO(001) [11] and BNFNO/Si(001) heterostructures (*f*).

MFES capacitor is

$$C_{\text{MFSM}} = \left(\frac{1}{C_{\text{Si}}} + \frac{1}{C_{\text{FE}}}\right)^{-1}$$

and in the case of $C_{\text{Si}} \gg C_{\text{FE}}$ (which is realized in the case of semiconductor surface enrichment with main charge carriers [14,15]) it is almost equal to C_{FE}. Preliminary experimental studies of the Au/BNFNO/Si(001) heterostructure have shown that at $U = \pm 10$ V the $C(U)$ dependencies have been observed that allowed making conclusions regarding the state of the MFES-structure due to the manifestation of the field effect [14,15] and calculating the $\varepsilon/\varepsilon_0$ of the FE material from values of E_{FE} at $T = -190\ldots200$°C. All $C(U)$ dependencies for the Au/BNFNO/Si(001) heterostructure had a form of high-frequency voltage-capacitance curve of MFES or metal–dielectric–semiconductor structures in the case of use of a *p*-semiconductor (examples are shown in Fig. 3, *a*–*e*). In the region of positive fields the transition of MFES-structures to a low-capacitance state took place (C_{min} less than 2.5 pF) caused by the contribution of the semiconductor when it transits to the state of depletion and inversion. In the region of negative fields, as the U grows the capacitance of the structure increases and achieves a plateau (C_{max} up to 35 pF), which is the capacitance of the FE-film (at these conditions the semiconductor surface is in the enrichment state). It is the C_{max} that has been further used to calculate $\varepsilon/\varepsilon_0$ of the BNFNO layer at $f = 50$ kHz in the aforementioned range of temperatures. The resulting $\varepsilon/\varepsilon_0(T)$ dependence in combination with similar dependencies for the BNFNO ceramics [16] and for the BNFNO/Pt/MgO(001) film [11] is shown in Fig. 3, *f*. In the BNFNO ceramics, a blurred maximum at $T_m \sim -70°$ was observed near the blurred ferroelectric → paraelectric (PE) phase transition. In the studied BNFNO film, the $\varepsilon/\varepsilon_0(T)$ dependence is similar, however the found unit cell strain in the material has resulted in a displacement of the region of FE → PE phase transformation toward high temperature region ($T_m = 31$°C). Dependencies with similar behavior took place in BNFNO/Pt/MgO(001) films as well ($T_m = 56$°C) [11], however in BNFNO/Si(01) the temperature stability of $\varepsilon/\varepsilon_0$ was significantly higher. The $\varepsilon/\varepsilon_0$ values in the produced film were lower as compared to BNFNO/Pt/MgO(001) [11] and were in the range of 95–130. Taking into account the fact that no impurity phases with low $\varepsilon/\varepsilon_0$ were observed in the produced heterostructure, we believe, that this is related to the polycrystalline structure of the film.

Ferroelectric properties of the BNFNO/Si(001) film have been analyzed by methods of scanning probe microscopy. The results of the investigation of lateral and vertical piezoresponse distribution for the BNFNO film are shown in Fig. 4. It can be seen from the experimental results that there is no lateral piezoresponse signal (Fig. 4, *c*) in contrast to the vertical piezoresponse signal (Fig. 4, *b*),

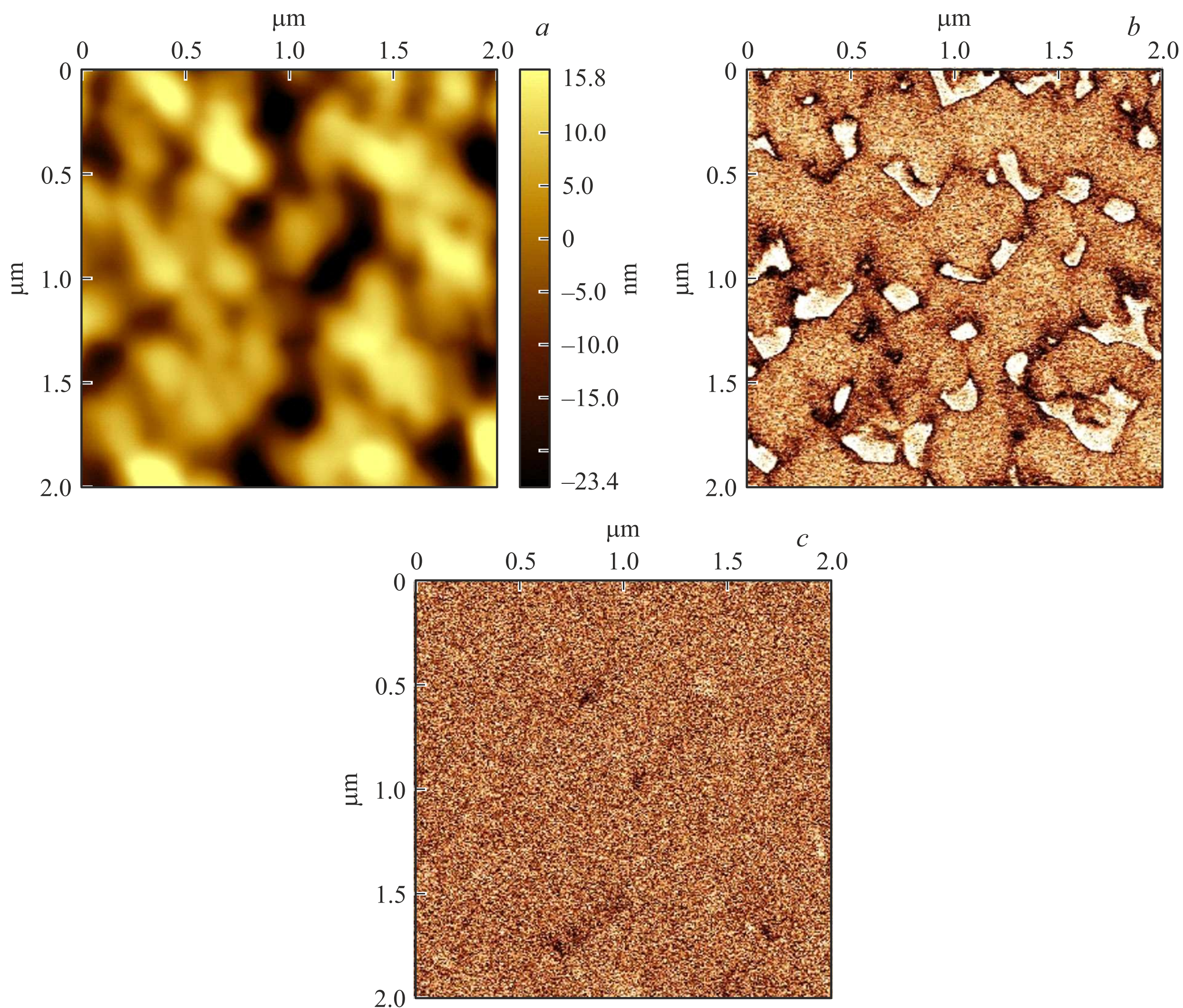

Figure 4. Image of topography (a), vertical (b) and lateral piezoresponse signal for the BNFNO/Si(001) film.

which is indicative of the presence of spontaneous polarization in vertical direction only. This confirms high degree of the film orientation along the [001] axis, the absence of impurity phases, which is consistent with the X-ray diffraction measurements. Experiments with the polarization of the films under study were conducted in the mode of piezoresponse force microscopy (Fig. 5) by applying negative (-10 V — „dark" region with a size of $5 \times 5\,\mu\text{m}^2$ in Fig. 5, b) and positive ($+10$ V — „light" region with a size of $2.5 \times 2.5\,\mu\text{m}^2$ in Fig. 5, b) voltages to the cantilever. After polarization, a „box-in-box" structure induced by the external electric field is visualized in the image of the piezoresponse signal, which confirm the ferroelectric nature of BNFNO/Si(001) films. At the same time, as can be seen from Fig. 5, a, nothing happens with the surface of barium-neodymium ferroniobate after the process of repolarization. In the mode of polarization switching spectroscopy a residual loop of piezoelectric hysteresis is obtained (Fig. 5, c). This also confirms the switching of polarization in the nanoscale region. It is worth to note that the obtained hysteresis loop is asymmetric about the axis of voltage, which is indicative of the presence of internal (built-in) voltage with a value of 0.45 V. Most probably, this was the reason for the initially small displacement of voltage-capacitance curves for the Au/BNFNO/Si(001) MFES-structure toward negative fields.

4. Conclusions

1. Based on the results of X-ray diffraction analysis and scanning probe microscopy it has been found that the BNFNO multiferroic films grown on the Si(001) substrate by the method of RF-cathode deposition in the oxygen atmosphere are c-oriented, single-phase and undoped films. The unit cell strain in the BNFNO film along the polar axis was 0.8% compared with bulk material.

2. with the analysis of the BNFNO film surface structure it has been shown that these films are characterized by a good homogeneity with a roughness of 15.39 nm, have no

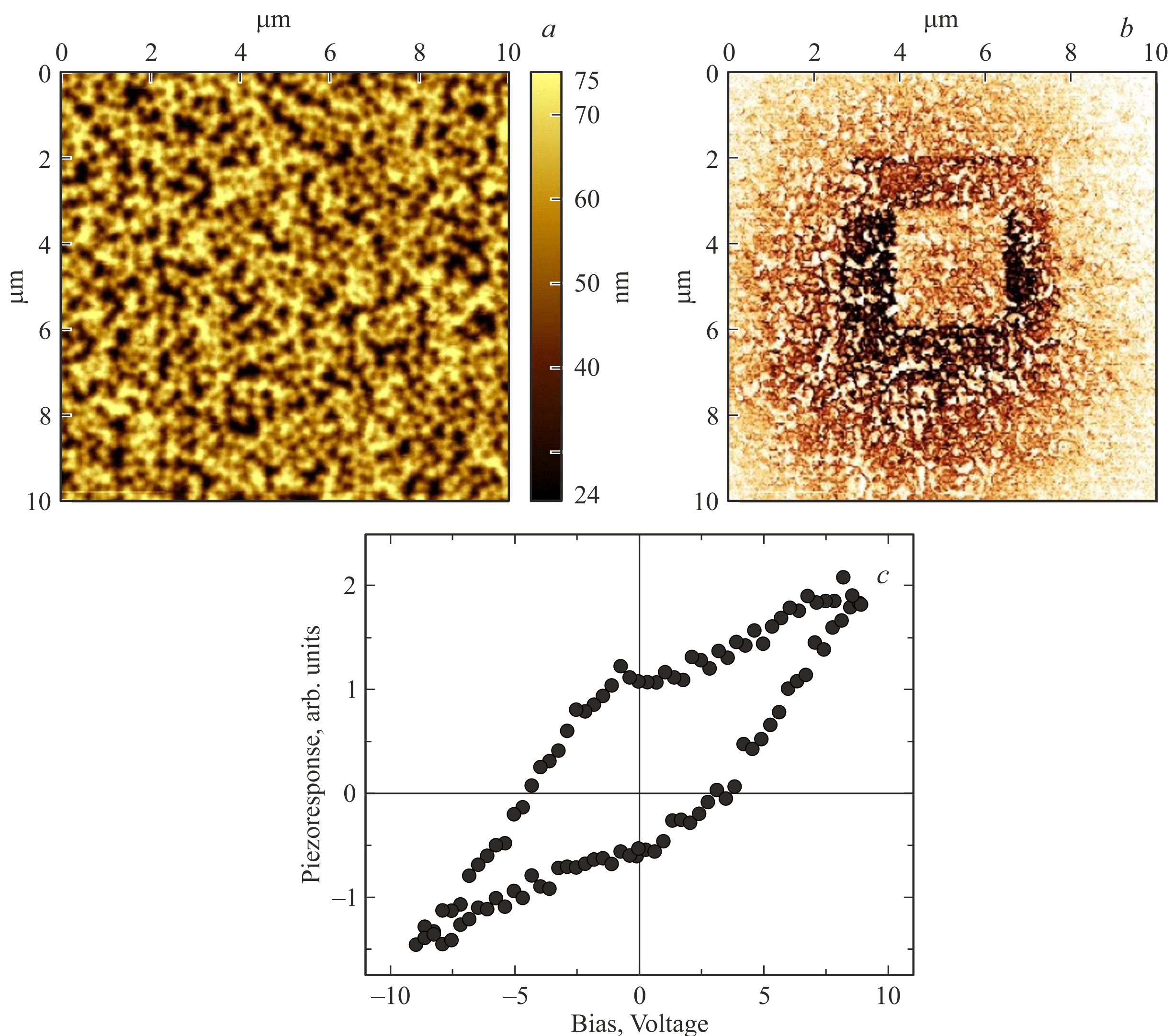

Figure 5. Topography (a), piezoresponse signal of induced domain structure (b), residual loop of piezoelectric hysteresis (c) for the BNFNO/Si(001) film.

pores, caverns, impurity phases and other defects on the surface, and the lateral size of crystallites evaluated by the method of autocorrelation function was ~ 134 nm.

3. Ferroelectric properties of BNFNO/Si(001) films at room temperature have been explicitly manifested through their analysis by the method of piezoresponse force microscopy and in the mode of polarization switching spectroscopy. In the range of $T = -190 \dots 150^\circ$C the permittivity of BNFNO varies from 95 to 130, at the same time, only one blurred maximum near 31°C is observed in the $\varepsilon/\varepsilon_0(T)$ curve.

4. The studies of vertical and lateral piezoresponse signals for the BNFNO film have shown that polarization in it is directed mainly along the normal to the film surface (there were almost no signs of polarization in the lateral plane).

5. It is reasonable to take into account the obtained results in the synthesis, investigations and development of functional elements based on undoped nanoscale films of BNFNO multiferroic, where the ferroelectric-to-paraelectric phase transformation takes place near the room temperature.

Funding

The study was performed with the support of the Russian Science Foundation grant No. 21-72-10180.

Conflict of interest

The authors declare that they have no conflict of interest.

References

[1] Yu.S. Kuzminov. Ferroelectric crystals to control laser radiation. Nauka, M. (1982). 400 p. (in Russian).

[2] A.V. Pavlenko, S.P. Zinchenko, D.V. Stryukov, A.P. Kovtun, Nanorazmernye plenki niobata bariya-strontsiya: osobennosti polucheniya v plazme vysokochasotnogo razryada, struktura i fizicheskie svoistva, Izd-vo YuNTs RAN Rostov n/D (2022), 244 p. (in Russian).
[3] T. Hajlaoui, C. Harnagea, A. Pignolet. Mater. Lett. **198**, 136 (2017).
[4] R. Bodeux, D. Michau, M. Josse, M. Maglione. Solid State Sci. **38**, 112 (2014).
[5] E. Castel, P. Veber, M. Albino, M. Velázquez, S. Pechev, D. Denux, J.P. Chaminade, M. Maglione, M. Josse. J. Cryst. Growth **340**, 156 (2012).
[6] M. Albino, P. Veber, S. Pechev, C. Labrugere, M. Velazquez, M. Maglione, M. Josse. Cryst. Growth Des. **14**, *2*, 500 (2014).
[7] V.M. Mukhortov, Yu.I. Yuzyuk, Geterostruktury na osnove nanorazmernykh segnetoelektricheskikh plyonok: poluchenie, svoistva i primenenie, YuNTs RAN, Rostov n/D (2008), 224 p. (in Russian).
[8] T. Hajlaoui, C. Harnagea, D. Michau, M. Josse, A. Pignolet. J. Alloys Comp. **711**, 480 (2017).
[9] R. Bodeux, D. Michau, M. Maglione, M. Josse. Mater. Res. Bull. **81**, 49 (2016).
[10] A.V. Pavlenko, T.S. Ilina, D.A. Kiselev, D.V. Stryukov, M.V. Ochkurov, FTT **64**, *6*, 658 (2022). (in Russian). DOI: 10.21883/FTT.2022.06.52391.286.
[11] A.V. Pavlenko, D.V. Stryukov, K.M. Zhidel, Ya.Yu. Matyash, Neorgan. materialy **58**, *10*, 1087 (2022). (in Russian).
[12] R.C. Munoz, G. Vidal, M. Mulsow, J.G. Lisoni, C. Arenas, A. Concha, R. Esparza. Phys. Rev. B **62**, *7*, 4686 (2000).
[13] A.V. Pavlenko, D.A. Kiselev, Ya.Yu. Matyash, FTT **63**, *6*, 776 (2021).
[14] J.J. Zhang, J. Sun, X.J. Zheng. Solid-State Electron. **53**, 170 (2009).
[15] L.S. Berman, FTT **35**, *2*, 200 (2001). (in Russian).
[16] A.V. Pavlenko, D.V. Stryukov. Ferroelectrics **590**, *1*, 220 (2022). https://doi.org/10.1080/00150193.2022.2037974

Translated by Y.Alekseev